*Article*

Modelling of Electric Power Generation Plant Based on Gas Turbines with Agricultural Biomass Fuel

Luis Fernando Rico-Riveros [1], César Leonardo Trujillo-Rodríguez [2], Nelson Leonardo Díaz-Aldana [2] and Catalina Rus-Casas [3,4,*]

1   Department of Electronic Engineering, Faculty of Engineering, Universidad ECCI, Bogotá 111311, Colombia; direccion.electronica@ecci.edu.co
2   Facultad de Ingeniería, Universidad Distrital Francisco José de Caldas, Bogotá 110231, Colombia; cltrujillo@udistrital.edu.co (C.L.T.-R.); nldiaza@udistrital.edu.co (N.L.D.-A.)
3   Department of Electronic and Automatic Engineering, University of Jaén, 23071 Jaén, Spain
4   Center for Advanced Studies on Earth Sciences, Energy and Environment CEACTEMA, Campus Las Lagunillas, University of Jaén, 23071 Jaén, Spain
*   Correspondence: crus@ujaen.es

Abstract: To ensure the survival of society, an enormous amount of energy is required to sustain the economic and social development of communities. In addition, there is a pressing need to achieve significant reductions in climate change and the associated costs of implementing systems based on traditional energy sources, as well as addressing the issue of providing electricity to isolated areas. In rural environments, there is an alternative energy source with enormous potential, agricultural biomass, which can produce electrical and thermal energy and can progressively help to reduce dependence on fossil fuels. The purpose of this work is to present a dynamic simulation model of a power generation plant that uses the Joule Brayton thermodynamic cycle, based on a gas turbine which is fueled by residual agricultural biomass; the cycle converts mechanical energy to electrical energy. The problem is approached through the characterization of the biomass, mathematical models of the plant components, and simulation of the system behavior in different scenarios. The simulations are processed in Matlab/Simulink, which allows the model to be verified, validating the equilibrium relationship between generation and load demand.

Keywords: integrated models; simulation; biomass plant; gas turbine; mechanical to electrical energy conversion

1. Introduction

Biomass power generation has been identified as an alternative for meeting future energy demand. As part of promoting the development of biomass technology, it is essential to understand the advantages and disadvantages of biomass technology, as well as the technological implementation of biomass plants and their start, operation and shutdown characteristics [1].

Over the last few decades, there has been a significant growth in biomass research, conversion technologies, and the end use of the products obtained. Within this growth is further progress in gasification, given the number of advantages it presents. Simultaneously to its development, this work has been carried out on different models that allow for better understanding, optimization, and management of this type of processes [2].

Mathematical modeling of a gasification process has proven to be a relatively fast and inexpensive solution compared to the direct construction of pilot units. Mathematical models, based on theoretical, experimental, and practical operational work, aim to analyze the thermochemical processes involved in biomass gasification and to evaluate the influence of the main input variables on the properties of the gaseous products (e.g., gas composition and calorific value). Different types of models have been developed for gasification systems,

including Computational Fluid Dynamics (CFD), Artificial Neural Networks (ANN), and thermodynamic equilibrium and kinetic models [3].

There is a large amount of work in the literature on gas turbine modeling [4]. The complexity of the model varies according to the intended application [5]. These models describe the spatially distributed nature of gas flow dynamics by dividing the gas turbine into several sections [6,7]. Mathematically, the complete description of the partial differential equation model boils down to a set of ordinary differential equations that facilitate application in a computer simulation program [4,8]. The simplest models for simpler applications, such as microgeneration, divide the gas turbine into only three sections corresponding to the main components of the turbine, i.e., compressor, combustion, and turbine [8].

Based on the referenced literature review and classification of studies presented, and focusing on energy generation through biomass plants and gasification processes with gas turbines, this work aims to develop a comprehensive model of an energy generation plant based on a gas turbine using agricultural biomass waste as fuel in a methodical manner. The model is simulated using the specialized software Matlab/Simulink.

The scope of this work is to verify the mathematical model through simulation, which will allow for continuity in subsequent developments towards the small-scale application of integrating a hybrid microgrid in a local environment in the department of Cundinamarca, Colombia. Therefore, the model must be comprehensive enough to represent the primary steady-state and transient characteristics of the plant, yet simple enough computationally to avoid complex implementation or long processing times during verification [4].

In this work, we implement models oriented towards the application of gas turbine-based microgeneration and highlight the relative simplicity of these models, which we verify mathematically and under simulation. The goals of this paper include: achieving control to stabilize variables at desired values, ensuring the necessary dynamic behavior when changing from one operating point to another, controlling fuel flow to achieve a desired load, controlling fuel/air ratio to provide the correct outlet gas temperature, and controlling injected water flow to prevent NOx emissions, as well as flow and temperature control.

The article is organized as follows. The materials and methods section presents a characterization of fuel based on agricultural biomass, references to studies based on models, a description of the used mathematical models, and a description of the control system and simulation model in Matlab/Simulink of the whole system.

Likewise, in the results discussion section, an analysis of the simulations carried out for various system test scenarios with variation in the load and fuel is presented. These variations are regulated by a classic PID control system, obtaining a satisfactory response for the biomass plant, generator, and control. The small-scale application of the mathematical models, plant modules, and control modules are verified, allowing the application to be oriented towards a projected integration of energy resources in a local microgrid in a non-interconnected area.

2. Materials and Methods

The following sections are presented in an orderly and consistent manner according to the development of consultation and application:

A. Characterization of fuel based on agricultural biomass;
B. References to model-based studies: thermodynamic, techno-economic, simulation, and mathematical;
C. Description of mathematical models;
D. Control system description;
E. Matlab/Simulink simulation model of the whole system.

A. Characterization of Biomass as fuel

Biomass means biological mass and corresponds to the amount of living matter produced on a given area of the earth's surface by organisms of a specific type [9]. The importance of biomass lies in the fact it can be transformed into energy, either electrical

or as a source of heat, given that organic substances are produced from plant matter, and when burned they produce energy and some other compounds such as CO_2 and water (H_2O). Biomass is classified into several types, depending on how it is constituted and its production sector. The types found are agricultural biomass, forestry biomass, livestock biomass, and Organic Urban Solid Waste (OUSW) biomass [10]. The use of agricultural biomass as fuel in a gas turbine plant has some important advantages, but also presents significant challenges that must be carefully considered; Table 1 summarizes some advantages and disadvantages presented by the use of agricultural biomass as fuel.

Table 1. Advantages and disadvantages of the use of agricultural biomass as fuel.

Source	Advantages	Disadvantages
[11]	Renewable energy source	May require processing
[12]	Reduction of greenhouse gas emissions	Combustion generates ash and tar
[13]	Waste reduction	Limited availability
[14]	Contribution to rural development	Requires space and resources
[15]	Local production	Can compete with food production

Source: Own.

Table 1 presents some characteristics of the advantages and disadvantages of the use of agricultural biomass residues as fuel. It can be seen that the advantages are that it is greater in terms of mitigating the environmental impact, the contribution of local economic developments in agricultural regions where there is a large amount of waste that can be processed and used, and using energy content as a renewable and sustainable resource.

The energy content of biomass is usually measured in terms of the calorific value of the resource. The calorific value of a fuel refers to the number of calories it is capable of producing by the combustion of a unit mass of each element. Not only biomass, but each fuel has an associated value against which it can be compared with others of similar characteristics [16].

The units are determined based on the state of the fuel, whether it is solid, such as firewood and agro-industrial waste, liquid, such as diesel, or gaseous [17,18]. The agricultural sector produces a significant amount of biomass [6]. In this sector, the by-products generated during the collection process are referred to as agricultural crop residues. For energy crops, plants that have fast growth and do not require much supervision for cultivation are usually used. Some crops, such as aquatic plants, soybeans, and peanuts, are used to produce biodiesel, while others, such as corn, cassava, wheat, and sugar cane, are used to produce bioethanol.

Table 2 shows the source of biomasses, the type of waste and their energy potential as a result of a characterization that was carried out in the Department of Cundinamarca in Colombia.

Table 2. Calorific value according to the crop.

Type of Crop	Type of Waste	LCV (kcal/kg)	Energy Potential (TJ/Year)	Energy Potential (GWh/Year)
Oil Palm	Fart	3.988	239.29	66.471
	Fibre	4.274	618.24	171.733
	Palm rachis	4.021	601.11	166.974
Panelera Cane	Bagasse	4.456	9524.84	2645.791
	Leaves—Bud	4.007	2866.22	796.173
Coffee	Pulp	4.259	217.76	60.489
	Cisco	4.430	100.73	27.981
	Stems	4.384	1165.21	323.67

Table 2. *Cont.*

Type of Crop	Type of Waste	LCV (kcal/kg)	Energy Potential (TJ/Year)	Energy Potential (GWh/Year)
	Stubble	3.429	318.01	88.336
Corn	Tusa	3.390	97.27	27.019
	Doormat	3.815	110.88	30.8
Rice	Tamo	3.113	143.98	39.995
	Husk	3.603	49.63	13.787
	Banana rachis	1.809	12.05	3.347
Banana	Banana stem	2.032	79.15	21.986
	Rejected banana	2.488	7.4	2.056
	Plantain rachis	1.808	10.03	2.786
Plantain	Plantain stem	2.032	65.88	18.3
	Rejected plantain	2.480	6.16	1.711

Source: [18].

Table 2 presents characterized values of the energy potential of crop and residue types, which depend on the climatic conditions of the agricultural area in which they are developed. This is an important criterion to consider when determining the availability of the residue with the highest energy potential that can be used. For example, in the study area of the department of Cundinamarca, Colombia, the most common crops are coffee, banana, and plantain. Table 2 shows that coffee stems have the highest energy potential. These models can be represented as mathematical functions that relate the different variables involved in the process, as shown in Table 3.

Table 3. The mathematical model for biomass characterization.

Equation	Parameter	Description	Value	Unit
$PE = M_{rs} * E$	PE	Energy Potential		[TJ/year]
	M_{rs}	Mass of dry residue		[t/year]
	E	Energy of the residue per unit mass		[TJ/t]
$M_{rs} = A * R_c * M_{rg} * Y_{rs}$	A	Cultivated area		[ha/year]
	R_c	Crop yield		[t main product/ha planted]
	M_{rg}	Mass of residue generated from the cultivation		[t of waste/t of main product]
	Y_{rs}	Dry residue fraction		[t dry residue/t wet residue]
$M_{RS} = \alpha * A * R_C * \sum_{i=1}^{n} \sum_{k=1}^{m} M_{rgki} * Y_{rski}$	"k" "i"	Biomass classification Types of waste biomass		[t/year]
	α	Unit conversion constant	1×10^{-6}	
$PE_{BRA} = \alpha * A * R_C * \sum_{i=1}^{n} \sum_{k=1}^{m} M_{rgki} * Y_{rski} * PCI_{ki}$	PE_{BRA}	The overall energy potential of agricultural waste biomass		
	PCI	Lower Caloric Value of the residue		[TJ/t]

Source: Own.

The mathematical models for assessing the energy potential of biomass are based on the fact that the energy contained in its matter is proportional to its dry mass.

The Lower Calorific Value (LCV) is defined as the amount of energy given off in the combustion of a unit of mass of a combustible material in which water is released as vapor. If this water condenses, it gives off heat, and the Higher Calorific Value (HCV) would then be obtained, adding this given-off heat to the LCV. Therefore, the LCV is lower than

the HCV, and the higher the moisture content of the fuel, the greater this difference will be. Therefore, the energy content of biomass is measured by the calorific value of the resource. It is necessary to clarify that the calorific value of resources, in the case of biomass, varies according to the level of humidity at which it is found. In particular, the higher the humidity, the lower the calorific value. In the case of biomass, it is necessary that the moisture content is less than 30% [19].

In many cases, the waste has a high moisture content, which requires conditioning, which is why the resources are usually subjected to prior drying processes, either naturally or induced, to make the raw material as suitable as possible for energy transformation processes [12].

The most suitable method to realize the energy utilization of agricultural biomass is through thermochemical processes. In the case of the agricultural sector, it must be taken into account that biomass residues contain a portion of the main product of the crop, and this fraction is usually larger than the unit [20].

Taking the LCV for different types of waste from different crops as a reference, the amount of biomass required to produce a certain amount of electricity can be dimensioned, for which calculations are presented in Table 4, taking generation as an example:

- Power required: 1 kW
- 1 kW = 860 kcal/h, equivalence
- PCI: 4.384 (kcal/kg). Average value of the PCI of the coffee stem taken from Table 2
- 1 cal = 4.1855 kJ, equivalence

Table 4. Calculation of the biomass required to produce electrical energy.

Equation	Parameter	Description	Value	Unit
$\text{Biomass}\left[\frac{kg}{h}\right] = \frac{\text{Power required}[kW]}{\text{PCI}[kcal/kg]}$	Biomass	Biomass quantity		$\left[\frac{kg}{h}\right]$
	Power	Power required		$[kW]$
	PCI	Lower Calorific Value		$\left[\frac{kcal}{kg}\right]$
$\text{PCI}\left[\frac{kcal}{Kg}\right] = 4.384\left[\frac{kcal}{Kg}\right] \times 4.1855[kJ]$ $= 18.349232\left[\frac{kJ}{kg}\right]$	PCI	Lower Calorific Value	4.384	$\left[\frac{kcal}{kg}\right]$
	cal	1 calorie	4.1855	kJ
	PCI $\ast$ cal	Product	18.349232	$\left[\frac{kJ}{kg}\right]$
$= 1[kW] \times 860\left[\frac{kcal}{h}\right] \times 4.1855[kJ] = 3599.53\left[\frac{kJ}{h}\right]$		Power required	3599.53	$\left[\frac{kJ}{h}\right]$
$\text{Biomass}\left[\frac{kg}{h}\right] = \left[\frac{3599.53\left[\frac{kJ}{h}\right]}{18.3492\left[\frac{kJ}{kg}\right]}\right] = 0.215\left[\frac{kg}{h}\right]$	Biomasa	Quantity of biomass required to produce 1 kW	0.215	$\left[\frac{kg}{h}\right]$

Source: Own.

With ideal efficiency values of the generation system of 100%, 0.215 kg/h would be required, but under an estimated lower performance, e.g., 90%, the following is obtained:

$$\text{Biomass}\left[\frac{kg}{h}\right] = \left[\frac{0.215\left[\frac{kg}{h}\right]}{0.9}\right] = 0.238\left[\frac{kg}{h}\right]$$

To produce 1 kW of power, 0.238 kg/h of agricultural biomass would be required, with an estimated efficiency of 90%.

B. References of studies based on different methods

The studies and references consulted based on different models, for a greater understanding of this work, are classified as follows: thermodynamic studies, techno-economic studies, studies based on simulation platforms, and studies of mathematical models. For

the first three, a brief reference is made, and for the last, which is the mathematical classification, a greater depth is presented, since the main objective of this work is to develop a complete mathematical model of a power generation plant based on a gas turbine whose fuel is agricultural biomass residue. Some references for each study are presented below.

References from thermodynamic studies. Table 5 presents some references based on the biomass gasification process, and energy, mass, exergy, chemical, and thermodynamic analyses.

Table 5. References of thermodynamic studies.

Source	Description	Process	Contribution
[2]	The complete evaluation of the thermodynamic performance of an integrated biomass-supported combined plant is investigated. For thermodynamic investigation, the mass, energy, entropy, and exergy balance relationships of the modelled plant and sub-plants are applied.	Biomass gasification	It performs a comprehensive thermodynamic calculation of the combined cycle supported by biomass gasification to produce electric heat, fresh water, and hydrogen.
[21]	Gasification modelling procedures fall into two main categories: equilibrium and kinetic models.	Biomass gasification	Develop a code using MATLAB software to apply the GA procedure for the purpose of system optimization from thermodynamic and economic perspectives.
[22]	It presents the simulation of a real mCHP plant, based on a biomass gasifier coupled to an internal combustion engine (ICE), in the Aspen Plus environment to predict the system behavior.	Biomass gasification	The model reproduces the operation of the syngas cleaning unit, the ICE, and the thermal recovery system. In particular, the thermal recovery system has been reproduced by implementing the detailed geometrical characteristics of the actual heat exchangers of the mCHP with Aspen EDR environment.
[23]	They propose computational fluid dynamics (CFD) simulation validated against experiments.	Biomass gasification	The results showed that all models can represent biomass combustion in a reasonable way. Biomass gasification is completed at a temperature of 1050 °K.
[3]	They develop and implement a zero-dimensional model for downdraft biomass gasification in fixed-bed or slow-bed gasifiers.	Biomass gasification	The proposed model considers the main gasification sub-processes (drying, pyrolysis, gasification) and their products. The model successfully predicts the conversion behaviors of different types of biomasses during a gasification process in terms of yield and product composition.

Source: Own.

References of techno-economic studies. Table 6 presents some references of studies, analyses, and case studies on the technological, economic, and environmental components aimed at energy sustainability using biomass gasification resources.

References of studies based on simulation platforms. Table 7 lists some references based on the use of specialized simulation software, and some other case studies oriented toward the knowledge and implementation of strategies and computational tools for optimization and modern control in biomass gasification processes are presented.

Table 6. References techno-economic studies.

Source	Description	Process	Contribution
[24]	The study shows that various techno-economic parameters have significant effects on the reduction of the normalized cost of electricity—LCOE in different power plant configurations.	CSP-biomass-TES hybrid power plant.	In the paper, they model and simulate three power plant configurations to calculate the cost of electricity for each.
[25]	They propose a novel concept of BECCS (Bioenergy with carbon capture and storage) for energy production.	Downdraft gasifier	The innovative energy system presented is defined based on the integration of a downdraft gasifier, an external combustion gas turbine, an MCFC section, an organic Rankine cycle and a cryogenic CO_2 capture. The proposed system is modelled and analyzed on the basis of exergy and exergy-economic analysis.
[26]	They evaluate the performance of an advanced biomass-fueled hybrid power generation system and model a modern biomass-based electrochemical power generation system.	Biomass gasifier, SOFC, Direct Combustion GT and ORC.	They present a detailed parametric study of the system to exhibit thermo-economic and environmental behaviors.
[27]	They present the latest statistical data on energy generation from bioenergy resources using available sources.	Biomass gasification	They include descriptions of gasification conversion routes, with their sustainability conditions, as well as the government policies necessary for their implementation in the Indian context.
[28]	A review of the sustainability aspects of biomass gasification and the use of biomass synthesis gas for small-scale power generation is presented, taking the UN Sustainable Development Goals (ODS) as a frame of reference.	Synthesis gas from biomass	The sustainability framework provided by the ODS, together with the concepts of energy transition and the energy trilemma, give bioenergy great importance in what should be its participation in an energy matrix geared towards distributed energy systems.
[29]	It assesses the feasibility of new renewable energy systems, and analyses the sustainability impact of these technologies along the entire supply chain in the environmental, social, and economic pillars.	Systems of Renewable energy	They consider not only the cost of energy but also the environmental and socio-economic impacts involved throughout the life cycle of the technology.
[30]	They present an analysis to achieve the EU's goals of a climate-neutral economy by 2050, highlighting that an adjustment of the current economy to one based on renewable raw materials (bioeconomic) must take place.	Bioeconomic	They stress that renewable solutions should be introduced into our existing production chain and should be conceived not as immediate solutions, but as long-term solutions, to be used as early as possible and improved over time.
[31]	They present an analysis of micro-scale biomass-fueled applications, with wood, straw, energy crop plants, and agricultural products being the most used fuels.	Applications Microscale	They study various types of boilers for each type of biomass, resulting from different fuel properties and investors' expectations (e.g., in relation to price and operational parameters such as the convenience of use).

Source: Own.

Table 7. References simulation platforms studies.

Source	Description	Process	Contribution
[32]	They point out that there are very few published studies on the modelling of biomass gasification based on the ANN method and even fewer in the field of fixed-bed downdraft gasifiers.	Biomass gasification based on the ANN method	They develop an integrated ANN model with a thermodynamic equilibrium approach for the downstream biomass gasification integrated power generation unit, which aims to predict the net power output of systems derived from various types of biomass feedstocks under atmospheric pressure and various operating conditions.
[33]	It presents an Artificial Neural Network (ANN) based model hybridized with a Particle Swarm Optimization (PSO) algorithm for a Biomass Gasification Plant (BGP) to estimate the amount of biomass needed to produce the syngas required to satisfy the energy demand.	Biomass gasification plant	The proposed model is compared with two traditional ANN models: Backward Feedback Propagation (FF-BP) and Forward Cascade Propagation (CF-P). ANNs are trained in MATLAB software using a real historical data set from a BGP located in the Distributed Energy Resources Laboratory of the Universitat Politècnica de València in Spain.
[34]	They researched about the possibility of using NARX ANN in a fixed-bed downdraft gasifier to predict syngas composition for lower data logging frequency.	Biomass downdraft fixed-bed downdraft gasifier	They obtain results from an open-loop network consisting of input and output layers connected with a hidden layer of 5 neurons. The application of the network allows online prediction and control of the gasification process.
[35]	They present two case studies that combining PV, biomass gasifier and batteries; one in Honduras and the other in Zambia.	Biomass gasification	The simulation resulting from the research allowed to review the performance of a gasifier in two HRES case studies that combine PV, biomass gasifier and batteries; one in Honduras and the other in Zambia.

Source: Own.

Mathematical modelling studies. Table 8 presents some references that are oriented toward mathematical modelling, simulation, and control, where the majority are based on the same models, but with different scopes of application in biomass gasification.

As has been mentioned, the main objective of this article is to develop the mathematical models of each component that is part of a gas turbine-based power generation plant. Although the other models which were consulted and referenced are important, it is considered that mathematical models are the basis for sizing. Simulating and evidencing behaviors of the components of the plant, and managing to establish a stable, reliable, and reproducible plant model, are the basis to determine and apply the other models. The referenced mathematical models are comprehensive enough to represent the primary steady-state and transient characteristics of the plant, yet simple enough computationally to avoid complex implementation or long processing times during verification.

The following section presents a detailed description of the mathematical models of each subsystem of the biomass-fueled gas turbine power plant.

C.   Description of the Mathematical Models

Gas turbines have played an important role in recent decades, due to their low initial investment cost and operational versatility. They can be used efficiently not only for emergency services to cover peak daily demand if required, but also as microgrid-based generation systems, which integrate energy resources into a comprehensive, manageable, and coordinated hybrid system.

Plants that use gas turbines to operate mechanical power, which is converted to electrical power by a generator, can operate either in closed or open loops. Figure 1 shows a schematic of an open loop gas turbine power plant.

Table 8. References mathematical models.

| Source	Description	Process	Contribution
[4]	The book presents comprehensive information on CC combined cycle and CHP combined heat and power cycle systems.	Biomass gasification	It presents in detail the mathematical, control, and simulation models of gas turbine, steam turbine, and combined gas turbine-based power plants. From the book the following references are highlighted [8,28,36–40], being the basis for the development and application of gas turbines.
[6]	The book presents comprehensive information on distributed generation using gas microturbines, apart from mathematical models, it highlights control models and microgrid applications.	Distributed electricity generation with gas microturbine	Control models and micro-grid oriented applications are highlighted.
[7]	In the Thesis, it is applied the dynamic models described in the book [27] by generating simulations of gas, steam, and combined cycle turbine plants, which validate the models for his own application.	Modeling and dynamic simulation of cogeneration schemes	It presents simulations of gas, steam, and combined cycle turbine plants, which validate the models for their own application.
[41]	It presents an application of mathematical models oriented to simulation and control based on neuro-fuzzy controllers, controlling several scenarios of variation of power, torque, active, and reactive load.	Neuro-fuzzy Control	Neuro-fuzzy controller applied to various scenarios of variation of power, torque, active, and reactive load.
[42–49]	They are based on the same mathematical and control models	Gas turbine	There is no great detail of the mathematical models, calculations, or parameters of each subsystem, each study focuses its development on specific applications.

Source: Own.
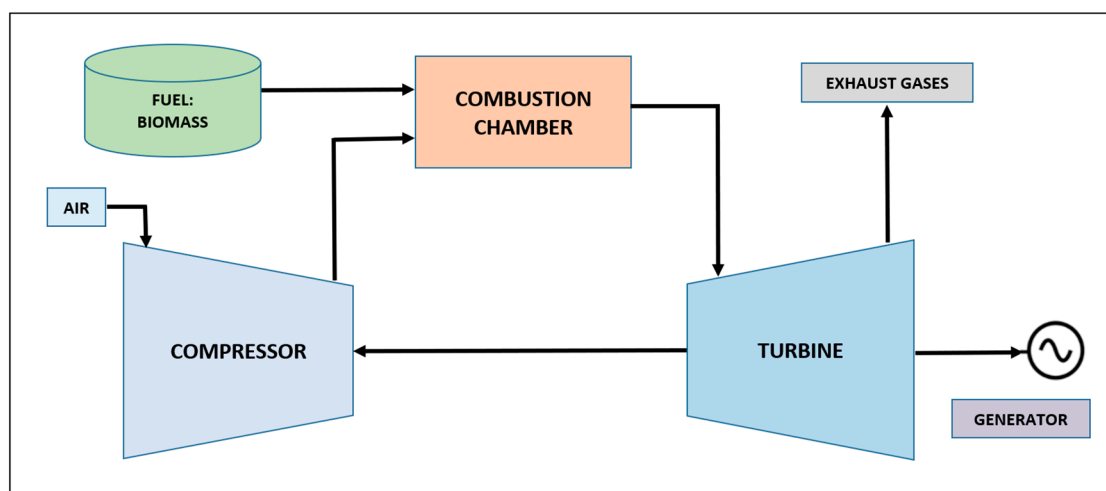
Figure 1. Open circuit gas turbine power plant. Source: [7].

In this configuration, fuel and air enter the combustion chamber and, after the chemical reaction is generated, the gas exits to the turbine producing mechanical power; the gases leaving the turbine are not recycled. This type of "open loop" plant does not constitute a thermodynamic cycle. However, its performance is often evaluated as if it were operating as a "closed loop" plant, Figure 2a illustrates this type of plant.
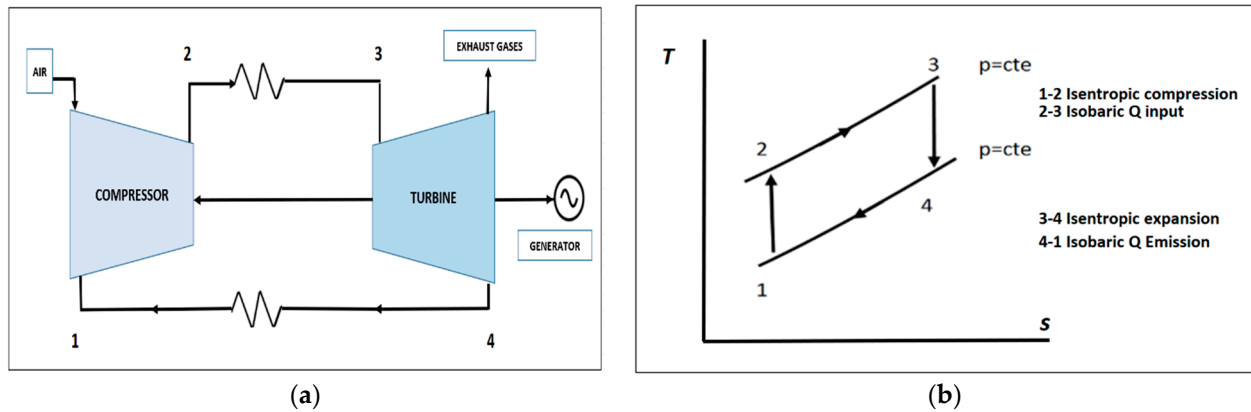

Figure 2. (**a**) Closed-loop diagram; (**b**) Temperature – Entropy *(T − S)* diagram of the thermal cycle of mechanical power generation with a gas turbine. Source: [7].

Power plants that utilize gas turbines are based on the constant pressure Joule Brayton cycle [28]. In this cycle, a constant flow of air or gas is compressed, heated, and expanded through the turbine, and then cooled in a heat exchanger, in the case of a closed thermal cycle. The turbine provides mechanical power to both the compressor and the generator.

In Figure 2, it can be seen that the main components of power plants using gas turbines are: the compressor, the combustion chamber, and the turbine. The way in which these plants operate is: at point 1, the air is taken from the atmosphere and enters the compressor to achieve the most favorable conditions for combustion. Then, at point 2, the air is mixed with fuel in gas form in the combustion chamber for combustion to take place, and then, at point 3, the hot gases that leave the chamber go to the turbine to produce mechanical power. In terms of energy conversion, the chemical energy that is released due to combustion is transferred to the gas flow. This energy, which is measured in terms of the enthalpy of the gases, is converted into mechanical power by the gas flow that turns the turbine. It must be considered that, in this process, part of the mechanical power which is handled goes to the compressor and the rest to the desired application.

In the T-s diagram of Figure 2b, the area under each of the process curves represents the heat transferred by that process; therefore, the area under the curve joining point 2 to 3 represents the heat transferred by the combustion taking part in the combustion chamber, as shown in Equation (1):

$$q_{ent} = \int_{s_2}^{s_3} T(s)_{2,3} ds \tag{1}$$

Equation (1) is valid for all processes, the limits of integration should be adjusted to the limits in which the process is carried out, and also the temperature as a function of entropy for that process. Then, the heat given off in the Joule Brayton thermal cycle is given by the area under the curve from 1 to 4, as shown in Equation (2):

$$q_{sal} = \int_{s_1}^{s_4} T(s)_{1,4} ds \tag{2}$$

Finally, by the first law of thermodynamics, the difference between the areas 2 and 3 and from 1 to 4 represents the net work produced in the thermal cycle, as shown in Equation (3):

$$W_{neto} = q_{ent} - q_{sal} \tag{3}$$

It is evident that the higher the temperatures handled in the 2 to 3 process and the lower the temperatures handled in the 4 to 1 process, the higher the efficiency of the thermal cycle.

In order to model the various components of gas turbine power plants, the following considerations are usually made [36,46]:

- Air and the products of combustion are considered ideal gases;
- The specific heats are considered constant for the products of combustion, air, and injected steam;
- The flow through the nozzles (compressor) is described as a polytropic, one-dimensional, and uniform adiabatic process;
- The energy storage and transport delay in the compressor, turbine, and combustion chamber are relatively small, which is why steady state equations are applied;
- The kinetic energy at the inlet of the gas flow in the compressor and turbine is considered negligible;
- The mass flow of air through the compressor is controllable by means of the blades at the inlet.

Taking into account the previous equations and considerations, more detailed information on the mathematical models resulting from analyzing the gas turbine as a process of compression and expansion of combustion gases (behavior of a nozzle) is presented below, for which the system is decomposed into four main subsystems. These are illustrated in Figure 3, where input, process, and output variables are highlighted.
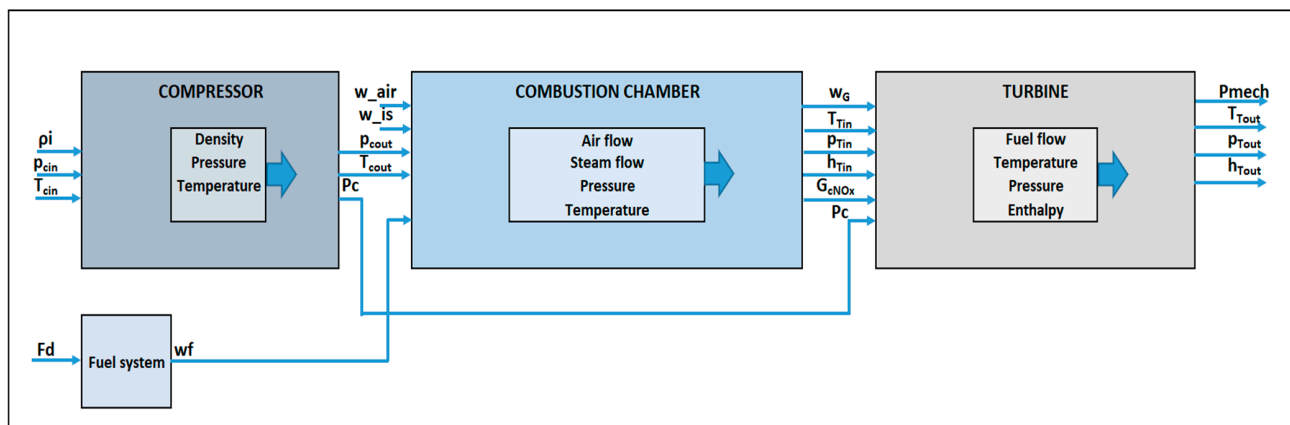

Figure 3. Gas Turbine Subsystems. Source: Own.

For the application and projected environments, a very high load requirement is not required, and all mathematical, simulation, and control models are dimensioned for the operation of a 5 kW power plant at a frequency of 60 Hz.

The mathematical models for the four (4) subsystems that make up the gas turbine-based power generation plant, as well as the electrical generator subsystem as a transducer of mechanical power to electrical power, are described below:

1. Fuel system (valve with actuator)
2. Compressor
3. Combustion chamber
4. Turbine
5. Electric generator

1. Fuel System

This system provides the fuel necessary for combustion to take place. In other words, from a fuel demand signal, this system operates by increasing the flow or decreasing the flow as required. The fuel flowing from the fuel system is the result of the inertia of the actuator and valve positioner, which are controlled by the PID controller's designer for this purpose. The equations in the Laplace domain, describing the dynamics of the system, are presented in Table 9, which shows: the equations, parameters, description, value, units, and procedure, as well as whether the value obtained arises from applying a calculation process, from a parameter, or from a constant.

Table 9. The mathematical model of the Fuel System.

Equation	Parameter	Description	Value	Unit	Procedure
$w_f = \frac{k_{ff}}{\tau_f S + 1} e_1$	W_f	Fuel mass flow.	2.889×10^{-4}	kg/s	Calculation
	k_{ff}	System Gain.	1	No Unit	Parameter
	τ_f	System time constant.	0.01	s	Parameter
	e_1	Valve positioner.	dynamic	No Unit	Calculation
$e_1 = \frac{a}{bS + c} e_2$	a, b, c	Valve parameters.	10, 1, 0	No Unit	Parameter
	e_2	Internal positioning signal.	dynamic	No Unit	Calculation
$e_2 = MF + F_d \omega_T e^{-S\tau} - w_f k_f$	MF	Minimum fuel signal.	0.8	p.u.	Calculation
	k_f	Feedback coefficient.	1	No Unit	Parameter
	F_d	Fuel demand signal.	1	p.u.	Calculation
	ω_T	Turbine speed.	188.45	rad/s	Calculation
	τ	System time delay.	0.01	s	Parameter

Source: Own.

2. Compressor

Compressors are positive displacement machines that maintain a constant volume in their chamber and a range of pressures at the outlet; the pressures depend proportionally on the inlet pressure to the compressor and are inversely proportional to the ratio of inlet-outlet densities. That is, the gas density at the compressor outlet is greater than the inlet density. The compressor is modelled as an equivalent nozzle in which an isentropic compression of the air is carried out, and the turbine as an equivalent nozzle in which an isentropic expansion of the gases leaving the combustion chamber is carried out, because this simplifies the models and, even with these simplifications, the relevant physics of the process, such as the change in temperature, pressure, and enthalpy, are still represented. Table 10 presents the mathematical model of the compressor.

The dynamics of the compressor are developed using the mathematical model outlined in Table 10. The following aspects can be observed: equations, parameters, descriptions, values, units, and procedures. The value obtained can arise from a calculation process, a parameter, or a constant. This model describes stable one-dimensional flow through the nozzle for uniform polytropic compression.

3. Combustion chamber

In this subsystem, combustion takes place where the hot gases, as a product of combustion, are directed to the gas turbine. The mathematical model of the combustor is presented in Table 11. The combustion of the gas turbine is modelled using the steady-state energy balance for combustion at the reference temperature.

4. Turbine

The turbine subsystem is where the gases leaving the combustion chamber expand. As the gases expand against the turbine blades, the turbine acquires kinetic energy, thus delivering mechanical power to the electrical generator.

Table 12 presents the mathematical model of the turbine, which is modelled using standard one-dimensional steady state gas flow equations.

Table 10. The mathematical model of the Compressor.

Equation	Parameter	Description	Value	Unit	Procedure
$w_a = $ $A_0 \left\{ \frac{2m_a}{\eta_{\infty c}(m_a-1)} (p_{cin}\rho_i) \left[(r_c)^{\frac{2}{m_a}} - (r_c)^{\frac{(m_a+1)}{m_a}} \right] \right\}^{0.5}$	w_a	Air mass flow inside the compressor.	5.767×10^{-1}	kg/s	Calculation
	A_0	Compressor outlet area.	1.2×10^{-2}	m²	Parameter
	$\eta_{\infty c}$	Polytropic compressor efficiency.	0.9	No Unit	Parameter
	ρ_i	Inlet air density.	1.21	kg/m³	Parameter
	p_{cin}	Inlet air pressure.	15.62	Pa	Parameter
	m_a	Polytropic index.	1.417	No Unit	Calculation
	r_c	Pressure ratio (p_{out}/p_{in}).	10	No Unit	Calculation
$m_a = \left\{ \frac{\gamma_a}{\gamma_a - \frac{(\gamma_a-1)}{\eta_{\infty c}}} \right\}$	γ_a	(c_{pa}/c_{va}) Specific heat ratio for air (constant).	1.411	No Unit	Calculation
	c_{pa}	Specific heat of air at constant pressure.	1.012	J/(kg °K)	Parameter
	c_{va}	Specific heat of air at constant volume.	0.717	J/(kg °K)	Parameter
$\left(\frac{p}{p_0} \right) = r_c = \left[\frac{2}{(m_a+1)} \right]^{\frac{(m_a)}{(m_a-1)}}$	r_c	Pressure ratio (p_{out}/p_{in}).	10	No Unit	Calculation
$p_{cout} = p_{cin} r_c$	p_{cout}	Outlet air pressure	156	Pa	Calculation
$\frac{T_{cout}}{T_{cin}} = (r_c)^{\frac{(\gamma_a-1)}{\gamma_a \eta_{\infty c}}}$	T_{cout}	Outlet air temperature	547	°K	Calculation
	T_{cin}	Inlet air temperature.	288	°K	Parameter
$P_c = \frac{w_{ain}\Delta h_I}{\eta_c \eta_{trant}}$	P_c	Compressor power consumption	1820	W	Calculation
	Δh_I	isoentropic enthalpy change. Corresponding to the compression of P_{cin} with respect to P_{cout}	2.698×10^5	J/kg	Calculation
	η_c	Total compressor efficiency.	0.863	No Unit	Calculation
	η_{trans}	Transmission efficiency from turbine to compressor.	0.99	No Unit	Parameter
$\eta_c = \left\{ \frac{1-(r_c)^{\frac{(\gamma_a-1)}{\gamma_a}}}{1-(r_c)^{\frac{(\gamma_a-1)}{\gamma_a \eta_{\infty c}}}} \right\}$	η_c	Total compressor efficiency.	0.863	No Unit	Calculation
$\Delta h_I = c_{pair} T_{cin} \left((r_c)^{\frac{R_{air}}{c_{pair}}} - 1 \right)$	c_{pair}	Specific heat of air at constant pressure.	1005	J/(kg °K)	Parameter
	R_{air}	Ideal gas constant for air.	287	J/(kg °K)	Parameter

Source: Own.

Table 11. Mathematical model of Combustion Chamber.

Equation	Parameter	Description	Value	Unit	Procedure
$w_G = w_a + w_f + w_{is}$	w_G	Outlet gas mass flow.	5.77×10^{-1}	kg/s	Calculation
	w_{is}	Steam mass flow injection.	2.9×10^{-5}	kg/s	Calculation
	w_f	Fuel mass flow to the turbine.	2.88×10^{-4}	kg/s	Calculation
$w_G c_{pg}(T_{Tin} - 298)$ $+ w_a c_{pa}(298 - T_{cout}) + w_f \Delta h_{25}$ $+ w_{is}c_{ps}(298 - T_{is}) = 0$		Equation for the energy of combustion at temperature 25 °C, is cleared for T_{Tin}.			

Table 11. *Cont.*

Equation	Parameter	Description	Value	Unit	Procedure
$w_G c_{pg}(T_{Tin} - 298) \quad +w_a c_{pa}(298 - T_{cout}) + w_f \Delta h_{25}$ $+ w_{is} c_{ps}(298 - T_{is}) = 0$	c_{pg}	Specific heat of flue gases	1144	J/(kg °K)	Parameter
	c_{ps}	Specific heat of steam.	2005	J/(kg °K)	Parameter
	c_{pa}	Specific heat of air.	1005	J/(kg °K)	Parameter
	T_{Tin}	Turbine inlet gas temperature.	1420	°K	Calculation
	Δh_{25}	Specific enthalpy of reaction at the reference temperature, (25 °C).	(-4.0×10^7)	J/(kg)	Parameter
	T_{is}	Steam temperature.	601	°K	Parameter
$p_{Tin} = p_{cout} - \Delta p$	P_{Tin}	Loss of combustion chamber pressure.	159	Pa	Calculation
$\Delta p = \left[\left(k_1 + k_2 \left(\frac{T_{Tin}}{T_{cout}} - 1 \right) \right) \frac{R}{2} \left(\frac{w_G}{A_m P_{cout}} \right)^2 T_{cout} \right]$	Δp	Loss of pressure in the combustion chamber.	2.698	Pa	Calculation
	k_1, k_2	Pressure loss coefficients	1	No Unit	Parameter
	R	Universal gas constant for flue gases	287	J/(kg °K)	Constante
	A_m	Cross-sectional area of the combustion chamber.	1	m²	Parameter
	T_{ref}	Reference combustion temperature.	1000	°K	Parameter
	h_{ref}	Reference flue gas enthalpy.	1.2×10^6	J/kg	Parameter
	h_{Tin}	Turbine inlet gas enthalpy.	1.685×10^6	J/kg	Calculation

Source: Own.

Table 12. The mathematical model of the Turbine.

Equation	Parameter	Description	Value	Unit	Procedure
$\frac{T_{Tout}}{T_{Tin}} = (r)_T^{\eta_{\infty T} \left(\frac{(\gamma_{cg} - 1)}{\gamma_{cg}} \right)}$	T_{tout}	Gas temperature at the turbine outlet.	763	°K	Calculation
	r_T	p_{Tout}/p_{Tin} Turbine pressure ratio.	6.29×10^{-2}	No Unit	Calculation
	p_{Tout}	Turbine outlet air pressure.	9.4	Pa	Calculation
	$\eta_{\infty T}$	Polytropic turbine efficiency	0.9	No Unit	Parameter
	γ_{cg}	c_{pg}/c_{vg}, Specific heat ratio for flue gases.	1.33	No Unit	Calculation
$w_G =$ $A_{T0} \left\{ \frac{2m_{cg}}{\eta_{\infty T}(m_{cg} - 1)} (p_{Tin}\rho_{Ti}) \left[(r_T)^{\frac{2}{m_{cg}}} - \left(\frac{p}{p_0} \right)^{\frac{(m_{cg}+1)}{m_{cg}}} \right] \right\}^{0.5}$	w_G	Turbine gas mass flow	5.77×10^{-1}	kg/s	Calculation
	A_{To}	Turbine outlet area	0.14	m²	Parameter
	$\eta_{\infty T}$	Polytropic turbine efficiency	0.9	No Unit	Parameter
	ρ_{Tin}	Inlet gas density	3.778×10^{-4}	kg/m³	Calculation
	p_{Tin}	Turbine inlet air pressure.	159	Pa	Calculation
	m_{cg}	Polytropic flue gas index.	1.384	No Unit	Calculation
$\rho_{Tin} = \frac{P_{Tin}}{R_{cg}T_{Tin}}$	ρ_{Tin}	Inlet gas density	3.778×10^{-4}	kg/m³	Calculation
$m_{cg} = \left\{ \frac{\gamma_{cg}}{\gamma_a - \frac{(\gamma_{cg} - 1)}{\eta_{\infty T}}} \right\}$	m_{cg}	Polytropic flue gas index.	1.384	No Unit	Calculation
$\left(\frac{p}{p_0} \right) = r_T = \left[\frac{2}{(m_{cg}+1)} \right]^{\frac{(m_{cg})}{(m_{cg}-1)}}$	r_T	p_{Tout}/p_{Tin} Turbine pressure ratio.	6.29×10^{-2}	No Unit	Calculation
$\eta_T = \left\{ \frac{1 - (r_T)^{\frac{(\gamma_{cg}-1)}{\gamma_{cg}}}}{1 - (r_T)^{\frac{(\gamma_{cg}-1)}{\gamma_{cg}\eta_{\infty T}}}} \right\}$	η_T	Overall turbine efficiency.	0.931	No Unit	Calculation

Table 12. *Cont.*

Equation	Parameter	Description	Value	Unit	Procedure
$\Delta h_I = c_{pg} T_{Tin} \left((r_T)^{\frac{R_{cg}}{c_{pg}}} - 1 \right)$	Δh_I c_{pg} R_{cg}	Isentropic enthalpy change. Specific heat of flue gas. Ideal gas constant for gas.	1.27×10^4 1144 287	J/(kg °K) J/(kg °K) J/(kg °K)	Calculation Parameter Parameter
$h_{Tout} = h_{Tin} - \eta_T \Delta hI$	h_{Tout}	Enthalpy of the turbine exhaust gases.	1.697×10^6	J/kg	Calculation
$P_T = \eta_T W_G \Delta hI$	P_T	Mechanical power delivered by the turbine.	6820	W	Calculation
$P_{mech} = P_T - P_c$	P_c	Power required by the compressor.	1820	W	Calculation
	P_{mech}	Net mechanical power available in the turbine.	5000	W	Calculation

Source: Own.

In addition to the description of the four subsystems of the plant, the mathematical model of the electric generator is presented.

5. Electric Generator

In order to convert the mechanical energy from the PGT into electrical energy, it is necessary to use an electric generator. Table 13 highlights some comparative advantages and disadvantages between synchronous and asynchronous generators [50]. This comparison allows for the establishment of a series of technical criteria in order to select the most suitable generator for the present application [51].

Table 13. Advantages and disadvantages of synchronous and asynchronous generators.

Advantages	Disadvantages
Synchronous Generator	
Greater efficiency	Greater complexity
Increased stability	Requires an excitation source
Lower long-term cost	Higher initial cost
Reactive power	Increased maintenance
Good power quality	Accurate grid synchronization
Low noise	Increased inertia
Greater responsiveness to load variations	Increased sensitivity to network disturbances
Accuracy in frequency control	
Asynchronous generator	
Simplicity	Lower efficiency
Does not require an excitation source	Lower power quality
Lower initial cost	Slower response time
No regular maintenance required	No regular maintenance required
Increased capacity to withstand network disturbances	

Source: [50,52].

Based on Table 13, and taking into account aspects such as efficiency, stability, power quality, greater responsiveness to load variations—which allows for greater precision in frequency control, and the parameter that relates to load requirements and fuel system control, it has been determined that the generator to be used in the simulation of the PGT plant is a synchronous generator whose equivalent in Matlab/Simulink is the Simplified

Synchronous Machine. Table 14 presents the mathematical model of the selected generator.

Table 14. The mathematical model of the Electric Generator.

Equation	Parameter	Description	Value	Unit	Procedure
$\Delta\omega(t) = \frac{1}{2H}\int_0^t (T_m - T_e)dt - Kd\Delta\omega(t)$ $\omega(t) = \Delta\omega(t) + \omega_0$	$\Delta\omega(t)$	Deviation from nominal operating speed	dynamic	rad/s	Calculation
	H	Inertia constant	3	s	Parameter
	T_m	Mechanical torque		N/m	Parameter
	T_e	Electromagnetic torque		N/m	Parameter
	kd	Damping factor	64.3	pu	Calculation
	$\omega(t)$	Mechanical rotor speed	188.45	rad/s	Parameter
	ω_0	Nominal operating rotor speed	188.45	rad/s	Calculation

Source: Own.

D.   Description of the control system

The gas turbine controller regulates both the gas turbine and the electric generator. One of the most popular designs is the SpeedTronic MarK IV system [39] developed for General Electric gas turbines. For the purpose of this article only, the control of the mechanical side of the gas turbine is the main focus; therefore, the model is significantly simplified.

The simplified model of the gas turbine controller is realized with a classic PID controller (supervisory), consisting of four inputs and three outputs. The inputs to the controller, which are outputs of the gas turbine model, are:

- Delivered mechanical power: Pmech, in W;
- Rotational speed (related to electrical frequency): ω in rad/s;
- Exhaust gas temperature: T_{Tout} in °K;
- Exhaust gas composition (NOx and CO content): g_{cNOx} in p.p.m.

The controller outputs that are inputs to the gas turbine model are:

- Fuel flow: conversion of fuel quantity Fd to p.u.;
- Air flow (inlet guide vane position): w_{air} in kg/s;
- Steam (or water) injection flow into the combustion chamber: w_{is} in kg/s.

Figure 4 shows the blocks of the control system, which consists of: PI controller for the electrical power signal Pe, PD controller for the rotational speed ω, P controller for the temperature signal T_{Tout}, PI controller of NOx gas emissions, and the LVF and MVF blocks which complement the system.

Each block of the control system is described below, and Table 15 presents the internal diagrams of each control block, as well as the parameters, description, value, and unit of each element that is part of each block.

- Power control Pe: this is implemented with the electrical power signal Pe coming from the generator GTP (Gas Turbine Plant); this in turn receives the mechanical power signal Pmech coming from all of the dynamics of the GTP. This signal is subtracted from the reference signal Pe_ref, and the result of the subtraction is integrated in the PI controller generating the required dynamic power signal according to the requirements of the load and the dynamic behavior of the other signals;
- Speed control: similar to power control, the rotor speed signal ω comes from the GTP generator and performs a similar procedure; it is subtracted from a reference value ω_ref, and the result of the subtraction is derived in the PD controller generating the required dynamic speed signal according to the requirements of the load and the dynamic behavior of the other signals. This control must be considered in safety conditions so that the turbine does not lose balance and overspeed;
- Temperature Control T_{Tout}: the temperature signal comes from the Turbine block, and the temperature value is the highest of the compression and expansion process that

occurs inside the plant; this parameter is important to control so that the temperature level does not exceed the upper temperature limit that the plant can withstand;

- Control of Outlet gases NOx: although a more robust and complex control of this block is not carried out, as it requires a deeper and more detailed development, it is important to take into account what it produces as a result in the outlet gases and pollutant components, as well as with the working temperatures; the behavior is reviewed as its process results in the steam flow of gases w_{is} are the steam mass flow injection;
- LVF Block (Minimum Value Selector): this allows discrimination of the lowest value signal coming from the power, speed, and temperature controls, with the power signal predominating, without disregarding the other signals that are considered more for plant safety procedures, in terms of speed overflow and temperature level overshoot;
- MVF Block (Maximum Value Selector): this also complements the system, as it allows the higher signal of the two incoming signals to pass, which are the ones coming from the LVF block and Fd_Mín; this last block is very important as it provides the minimum flow signal that must be injected to the plant so that it does not shut down and maintains the flame of the combustion system.
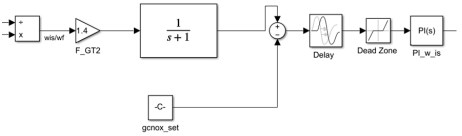
E. Matlab/Simulink simulation model of the whole system.

By interconnecting all the subsystems developed up to this point, we have an equivalent that involves the fuel flow input, which will come from a controller and the mechanical power as output; this concept is illustrated in Figure 5. All the subsystems obtained can be part of an equivalent system, in which only the fuel flow is required as input and the mechanical power and the gas temperature parameters at the turbine outlet as output. Through the mechanical power, the generator system based on a simplified synchronous machine is connected.

Table 15. Gas Turbine—Generator PID Control Model.

Control	Parameter	Description	Value	Units
Electrical Power: Pe	Pe_pu	Signal power generator	1	p.u.
	Pe_set_pu	Reference signal generator power		
	PI_Pe	Proportional—Integral		
	P	Proportional		
	I	Integral		
Rotor Speed: ω	ω_pu	Rotor speed of operation		p.u.
	ω_set_pu	Reference rotor speed of operation		p.u.
	PID_ ω	Proportional—Integral—Derivative		
	P	Proportional		
	I	Integral		
	D	Derivative		
Temperature: T_{Tout}	T_Tout_pu	Turbine outlet temperature		
	Función CR	Radiation field		
	T_Tout_set_pu	Outlet reference temperature Turbine		
	FunciónT	Termocouple		
	P_T_Tout	Proportional_T_Tout		
	P	Proportional		
	PI_w_air	Proportional—Integral airflow		
	P	Proportional		
	I	Integral		

Table 15. *Cont.*

Control	Parameter	Description	Value	Units
Gases NOx: g$_{cNOx}$	**g$_{cNOx}$**	Mass flow of NOx		
	w_{is}	Steam mass flow inyection.	2.9×10^{-5}	kg/s
	w_f	Fuel mass flow to the turbine.	2.88×10^{-4}	kg/s
	f$_{GT2}$	Experimental curve: NOx steam mass flow to fuel ratio		
	g$_{cNOx\_set}$	Reference mass flow of NOx		
		Delay	0.001	
		Dead Zone	−0.1–0.1	
	PI_w_is	Proportional—Integral mass flow of steam		
	P	Proportional	0.0002	
	I	Integral	0.001	

Source: Own.
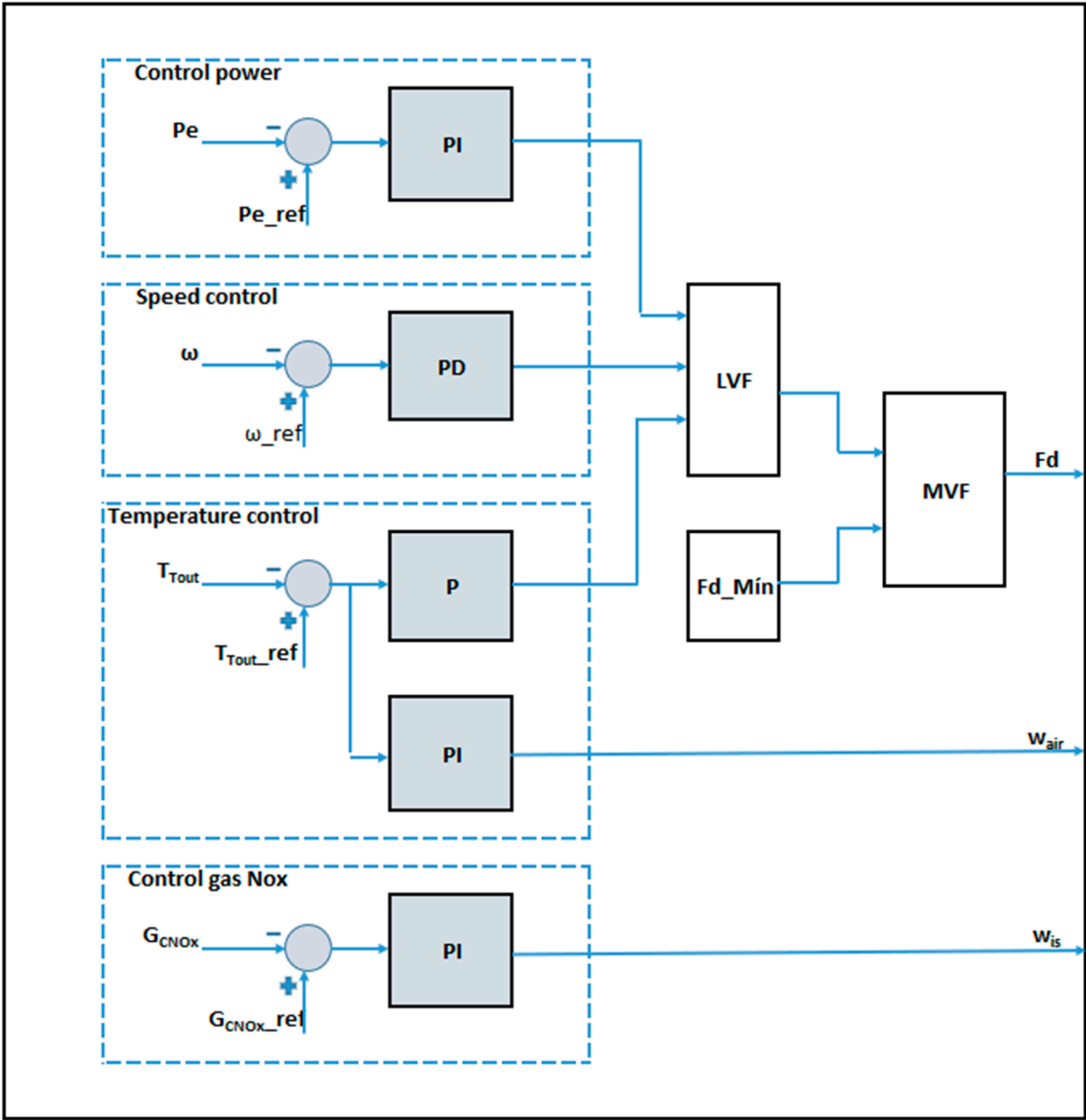
Figure 4. Control system blocks. Source: Own.
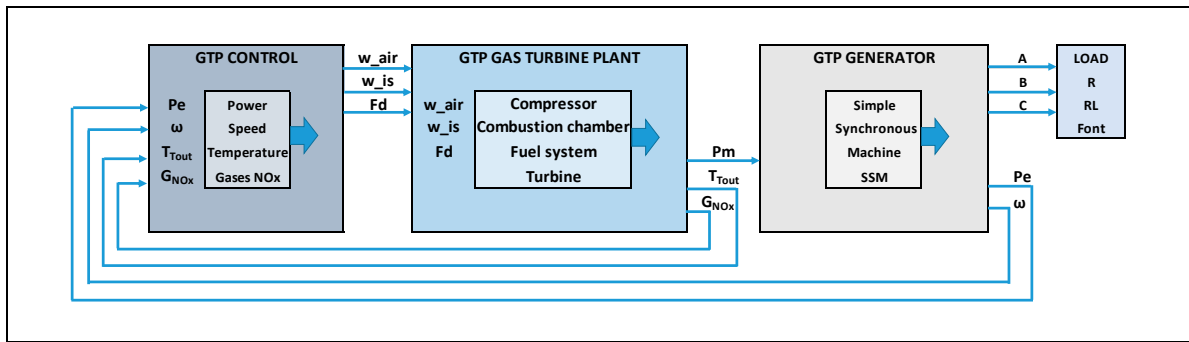
Figure 5. Blocks of the whole system: GTP control, GTP Plant, GTP generator and load. Source: Own.

As a result of the procedure described above, in terms of the implementation of all the models, in the first instance, all the mathematical models were transferred to Excel for monitoring, verification, and interaction of each equation for each component that is part of each subsystem. The appropriate dimensioning and parameterization were carried out on a small scale for the application of a 5 kW full-scale generation plant. From the monitoring and verification in Excel, all the models were implemented in Matlab/Simulink. Figure 6 shows the implementation in blocks of each component of the GTP system with fuel characterized as agricultural biomass residue.
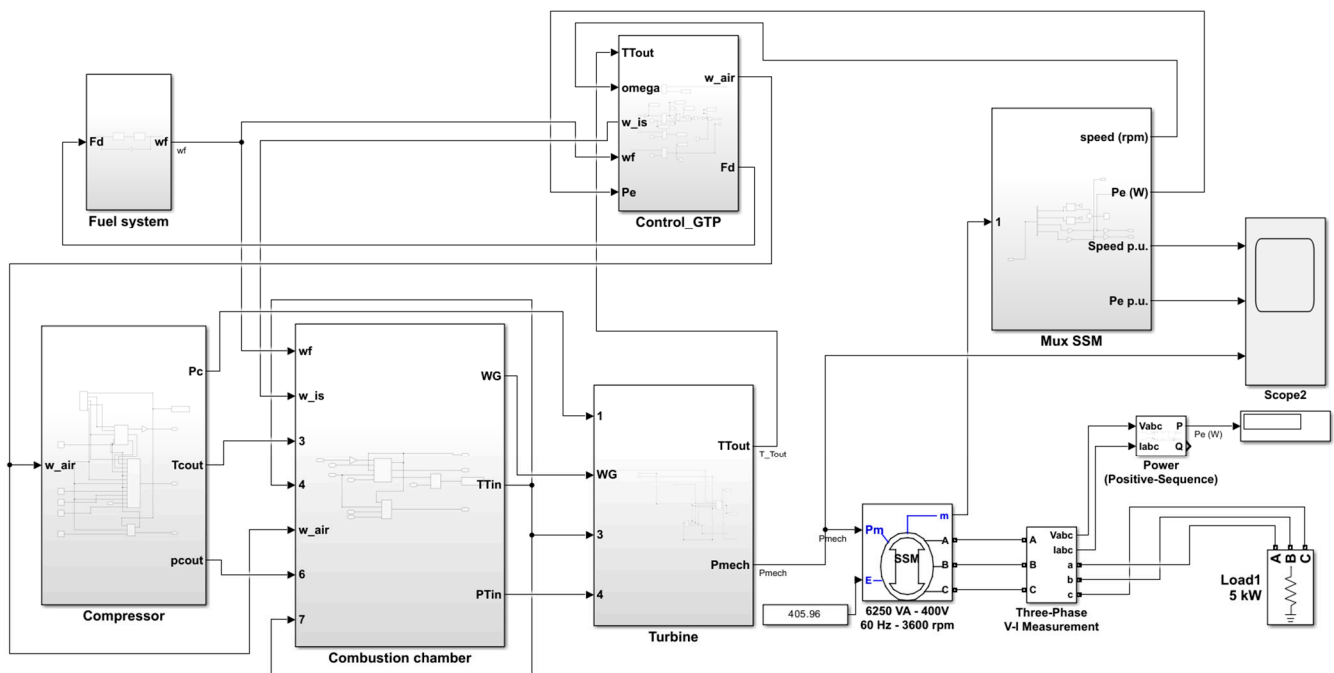
Figure 6. Matlab/Simulink model: GTP control, GTP plant, GTP generator and load. Source: Own.

The sub-systems are listed below:

1. GTP Control (Gas Turbine Plant);
2. Fuel System;
3. Compressor;
4. Combustion Chamber;
5. Gas Turbine;
6. Simple Synchronous Machine (SSM);
7. Simple Synchronous Machine (SSM) output multiplexer: speed in rpm, electrical power Pe (W);
8. Three-phase outputs;

9. Three-phase resistive load.

3. Discussion of Results

According to the entire procedure developed for the implementation and verification of the mathematical models of each of the subsystems described and which constitute the GTP-based generation plant, two generalized scenarios are presented for the verification of the results, which are aimed at operating with resistive load for basic consumption in a rural domestic environment. The scenarios are described below:

1. Checking of nominal values:

In this scenario, there is variation in the load requirement, which leads to fuel variation. Figure 7 shows the load variations of a 1 kW and 5 kW requirement. For simplification of the calculations and presentation of the data, the parameterization and conversion of the SI international average system to parts per unit p.u. is used, corresponding to the parameterization of 5 kW to 1 p.u., 4 kW to 0.8 p.u., and so on until a value of 1 kW corresponding to 0.2 p.u. is obtained.

As an example of checking the low nominal value, Figure 7a shows the variation in the load requirement of 1 kW. The red graph illustrates the mechanical power output of the GTP, denoted as Pmech, with the conversion of units for a 1 kW variation of 0.2 p.u. being obtained. Similarly, the blue graph represents the output of the Simple Synchronous Machine, also demonstrating a variation of 0.2 p.u.
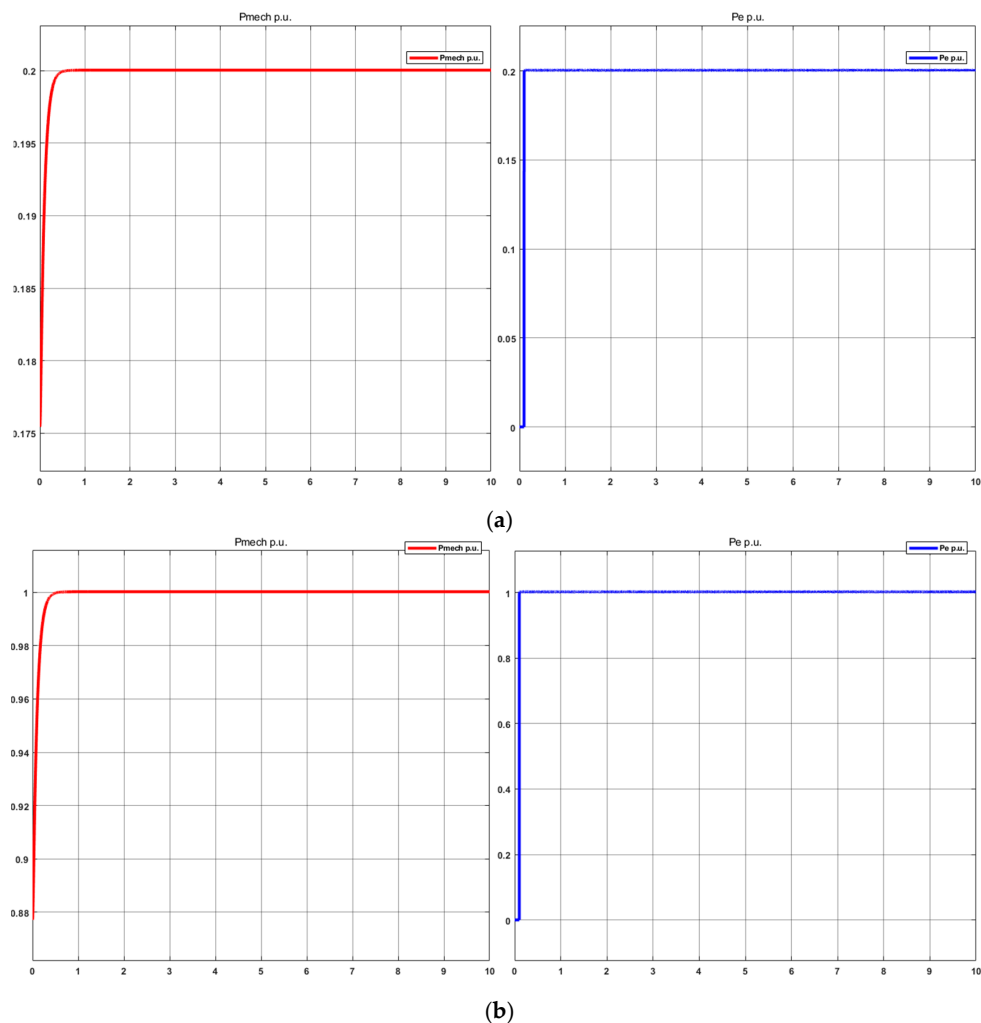

(a)

(b)

Figure 7. 1 kW and 5 kW load requirement with varying Pmech and Pe. (**a**) 1 kW load requirement, (**b**) 5 kW load requirement. Source: Own.

For the case of variation in the highest nominal value, Figure 7b represents the variation in the load requirement of 5 kW, the red graph illustrates the mechanical power Pmech being the output of the GTP, with the conversion of units for a 5 kW variation of 1.0 p.u. being obtained. Likewise, the graph in blue represents the output of the Simple Synchronous Machine, also representing a variation of 1.0 p.u.

For the two example cases, when there is variation in the load requirement, there is a correspondence in output variation in both the GTP and the Simple Synchronous Machine. The operation of the integration and interaction of the generation plant based on a gas turbine and electric generator is checked for the nominal values of 1 kW and 5 kW.

From Figure 7, it can be seen that, in general the operation of the GTP can be checked and verified, given the load requirement. In the plant, a dynamic occurs in the subsystems and in the control system when there is a load requirement. When the load requirement occurs, it generates an electrical power requirement and rotor speed variation requirement, which is detected by the control system of each of these variables, as presented in the previous section; in the dynamics of the PID controller the amount of fuel flow required for each case is determined.

2. Dynamic load requirement variation:

The dynamic response of the modelled and implemented system with dynamic behavior is tested in the transitions of load variation in an upward and downward manner. Figure 8 shows the variations every 10 s, from 1 kW to 5 kW upwards and load variation from 5 kW to 1 kW downwards. Every 10 s there is a load change transition of 1 kW; the scenario starts at 0 and, after 10 s, the load varies for a consumption of 1 kW, then, after another 10 s, the load requires a consumption of 2 kW. This variation continues until 50 s, when it reaches full load with a consumption of 5 kW.
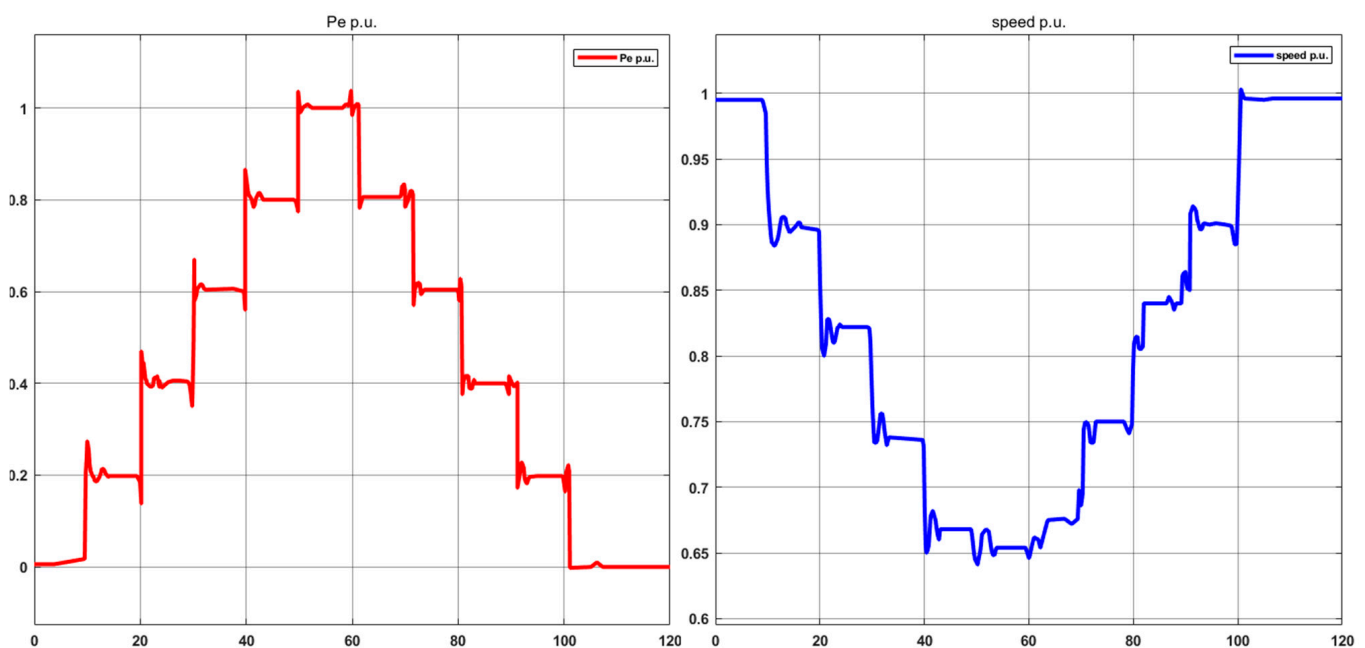

Figure 8. Variation in load requirement—variation in rotor speed. Source: Own.

Likewise, the dynamic response of the system in a downward manner is checked in the transitions of load variation from 5 kW to 1 kW, where every 10 s a transition of 1 kW load change is made. The scenario is reversed after 60 s when switching to a load for a consumption of 4 kW, then, after another 10 s the load requires a consumption of 3 kW, and this variation continues until 100 s when it is allowed to have no load.

Figure 8 shows the dynamic behavior with the transitions described above for the variation in electrical power Pe (p.u.) in the red color and speed variation (p.u.) in the blue

color. When carrying out these variations, the measurements on the *y*-axis are made in p.u. and the *x*-axis is the time variation. Each variation in the load requirements corresponds to a variation of 0.2 p.u., corresponding 1 p.u. to the load requirement of 5 kW and so on for the other transitions until 0.2 is obtained, which corresponds to a load requirement of 1 kW. The integration and interaction of the generation plant based on a gas turbine and electric generator is tested for the nominal values of 1 kW, 2 kW, 3 kW, 4 kW, and 5 kW.

Table 16 presents information for all nominal test values, where the operation of the whole system is characterized, taking the values of: load variation (power, W), transition time between ascending states (seconds, s), transition time between descending states (seconds, s), fuel flow variation (wf, kg/s), air flow variation (wa, kg/s), and steam mass flow variation (w_{is}, kg/s), with these flow variables being the ones that provide the dynamic behavior of the whole system.

Table 16. System characterization with load variation, response times, and flows.

Load (W)	Upward Transition Time (s)	Downward Transition Time (s)	wf (kg/s) Fuel Flow	w_a (kg/s) Airflow	w_{is} (kg/s) Steam Mass Flow
1000	3.5	1.4	5.77938×10^{-5}	0.115351848	5.80188×10^{-6}
2000	5.2	3.7	0.000115588	0.230703695	1.16038×10^{-5}
3000	3	2.5	0.000173381	0.346055543	1.74056×10^{-5}
4000	4	3.5	0.000231175	0.46140739	2.32075×10^{-5}
5000	3.1	3.5	0.000288969	0.576759238	2.90094×10^{-5}

Source: Own.

From the graphs in Figure 8 and the data obtained in the simulations presented in Table 16, it can be determined that:

- The average settling times for state transitions resulting from variations in the load requirement of a 1 kW are: 3.76 s for up states and 2.92 s for the down states, with the times being slightly lower for down states;
- Although the dynamic behavior of the flows referenced in Table 16 shows a certain regularity and proportionality oriented towards a linear behavior, these behaviors are not reflected in the establishment times; because a more stable system is not available for these variations, work continues on the regularization of the control strategies used;
- There is a logical behavior in the fuel flow consumption, which is reflected in the variation in the air flow and mass flow, as more fuel flow is required when there is a higher load requirement, and with the opposite behavior being observed when there is a lower load requirement, requiring less fuel flow, air flow, and mass flow of steam;
- The rotor speed variation in the simple synchronous machine presents more irregularities due to the behavior of the non-linear parameters of the mathematical model, which are translated in the simulation into more abrupt changes due to the transitions in the load requirement states. The control strategies must be able to linearize the damping factor and the deviation from the nominal operating speed.

3. Contrast variation in consumption profile and plant model

For the presentation of this scenario, indicators of official demand forecasts are taken as a reference on the website of the company xm [53], and they can be consulted and downloaded to find the information regarding the monthly balance of the indicators of the official forecast of the demand of the NES (National Electric System) according to regulations of the National Council of Operations through Agreement NCO 1303 [54]. The NES and NCO are governmental organizations of Colombia, and in the consulted files, information can be found on the consumption provided by the company Codensa S.A.

ESP (Company of distribution and commercialization of electric energy, provider of public services especially in the regions of Bogotá and Cundinamarca in Colombia) [55].

To meet the load requirement of the GTP in this scenario, the consumption variation from the reference file was adjusted to match the plant's load variation, allowing for a realistic simulation of the load profile behavior. Simulations were carried out for all seven days of each week in February 2023. As an example, Figure 9 shows an Excel graph representing the consumption variation in kW for Wednesdays, while Figure 10 presents the simulation results using Matlab/Simulink for the same day. The consumption variation is presented in p.u. and the simulation duration was 240 s.
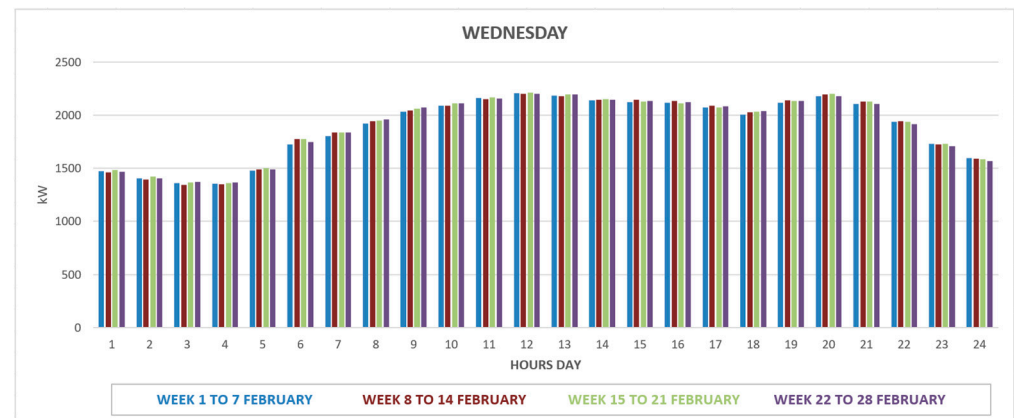
Figure 9. Variation in consumption reference file—Codensa for Wednesdays of the month of February 2023.
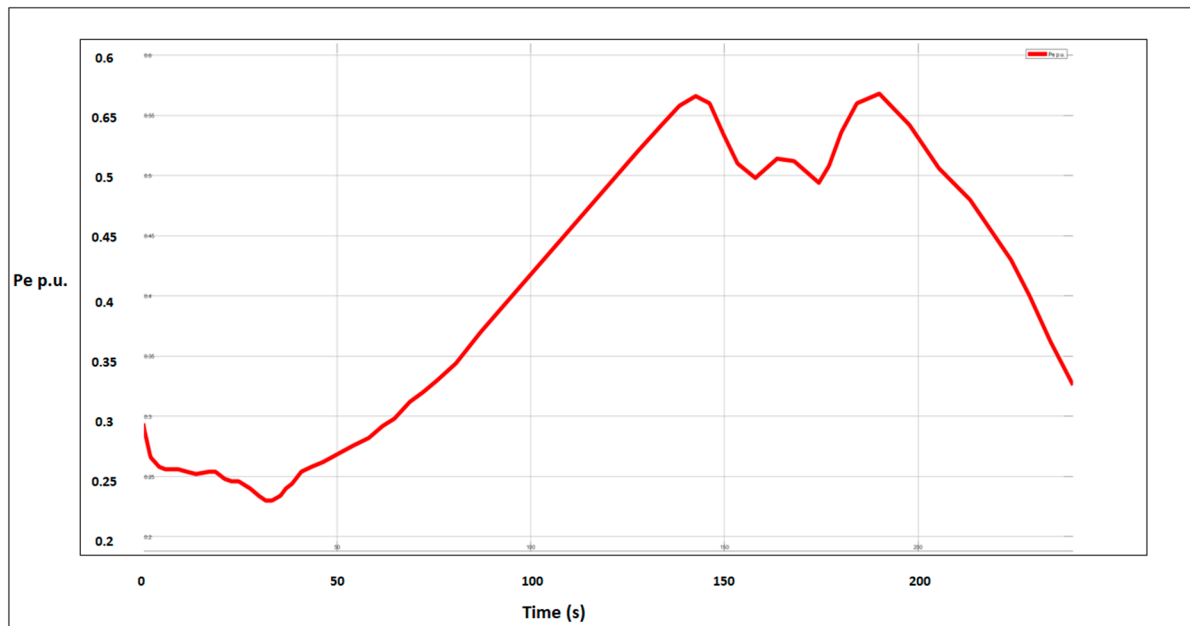

Figure 10. Simulation of consumption variation based on reference file—Codensa. Source: own.

Table 17 presents information on the variation in the consumption profile of the file taken as a reference. The values of load variation in W are presented, as well as the values of load variation in the simulation. These values are shown in their equivalent in p.u. and, according to the load variation, the variations of fuel flow (w_f, kg/s) are presented alongside variation in air flow (w_a, kg/s) and variation in steam mass flow (w_{IS}, kg/s). These flow variables are those that provide the dynamic behavior of the entire system.

After reviewing and monitoring the variation in consumption in the behavior generated in Figures 9 and 10 and Table 17, the following changes in consumption are observed from the actual load profile of the simulation taken from the reference file:

- There is a drop in load from hours 1 to 4, which is observed in the simulation between 0 and 40 s;
- From hour 5 to hour 12 in the Excel graph and from 50 to 150 s in the simulation, there is a higher demand for load;
- From 13 to 18 h, there is a decrease in the demand for load, which is also observed in the simulation between 130 and 180 s;
- There is an increase in consumption again between 18 and 20 h, which is observed in the simulation between 180 and 190 s;
- Finally, from hour 21 to 24 and from 190 to 240 s in the simulation, there is a drop in the demand for load.

Table 17. Example consumption profile variation applied to simulation.

Hour Day	Load Variation in W Reference File Figure 9 (W)	Load Variation in p.u. of the Simulation in Figure 10 (p.u.)	w_f (kg/s) Fuel Flow	w_a (kg/s) Airflow	w_{is} (kg/s) Steam Mass Flow
1–4	1486	0.3	0.0000858815868	0.1714128455336	0.00000862159368
	1360	0.26	0.000078599568	0.156878512736	0.0000078905568
5–12	1499	0.3	0.000078599568	0.1729124195524	0.00000869701812
	2201	0.55	0.0001272041538	0.2538894165676	0.2538894165676
13–18	2194	0.57	0.0001272041538	0.2530819536344	0.2530819536344
	2034	0.48	0.0001175525892	0.2346256580184	0.2346256580184
18–20	2034	0.48	0.0001175525892	0.2346256580184	0.2346256580184
	2202	0.56	0.0001272619476	0.2540047684152	0.2540047684152
21–24	2127	0.45	0.0001272619476	0.2453533798452	0.2453533798452
	1587	0.38	0.0000917187606	0.1830633821412	0.00000920758356

Source: own.

It should be noted that the consumption variations presented in the reference file are taken and followed by the plant simulation.

Comparing the graphs in Figures 9 and 10, although there are some peak values that deviate slightly in the simulation, it can be determined that the plant model generally produces variations in the simulation that correspond with those presented in the reference Excel file values.

The behavior of the variables is verified according to the plant models in tracking the variation in consumption per hour on Wednesdays, which are taken as reference values.

Of the results obtained in terms of the verification of the models in the scenarios in the simulations, the applied methodology is highlighted, of which the following stand out:

1. A classification of the studies consulted is proposed and generated, whether they are thermodynamic, techno-economic, based on simulation with specialized software, and mathematical, which is the main object of this work. The proposal is made in this way because, in all of the reference consultations, no differentiation is made, which generates confusion and mixture between models, which does not indicate that the models discard each other;
2. Mathematical verification of each equation implemented in each subsystem of the plant, initially in Excel and later in Matlab/Simulink in the simulations which were carried out.
3. Detailed presentation of all mathematical models, with equations, parameters, and values obtained if they are calculations, constants, and units. In most references which were consulted, especially articles, no further details of the models can be found;

4. Results were obtained for a proposal for small-scale generation, facilitating sizing, where the gas turbine model is the most suitable plant option for these applications, as it provides fewer complex calculations, dynamics, and control. The mathematical model was mostly linear with the application of algebraic equations, and the most dynamic sequences are found in the fuel and control systems;

5. The load requirements determine the fuel flow requirements, which affects the air and steam mass flows; consequently, it also affects the mechanical power, electrical power, rotor speed, and transition times both up and down, affecting the stability and reliability of the system. To improve this behavior, the responses of the control strategies must be further adjusted and sensitized;

6. For an integration application in a hybrid microgrid where more energy resources are involved, control strategies more akin to a management system must be considered and developed.

4. Conclusions

In the GTP modeled and simulated under several test scenarios, the electric power generation system was able to prioritize the balance relationship between generator and load, controlling the flow of fuel in all of the situations which were experienced.

It was found that the variation in the fuel flow is determined by the variation of the load, influencing the variation in rotor speed and variation in electrical power, which are both variables that were controlled, generating stability, repeatability, and reliability in the tests and experimental results.

From the results of the simulation, it is obtained that, in the plant, the variation in rotor speed is constantly corrected; when presenting an increase or decrease in this speed, the control system that relates the power and demand are balanced, correcting the situation when the power is above the demand, or otherwise when the power production is not sufficient for the demand. Consequently, in the results of the simulations, it was possible to stabilize the speed, with that being one of the main tasks of the plant control system.

As a control strategy, classical P, PI, and PD controllers were implemented. For the application of this article, they were adopted and adapted through adjustments to the small-scale requirements that were carried out. In the results which were obtained, these controllers provided safe and fast operation. However, it is appreciated that, for the requirements of plants with greater complexity, the performance of other more robust control techniques can be explored.

The objective of verifying the mathematical models of the plant in their implementation and testing through the scenarios proposed in the simulations has been achieved, but we are aware that adjustments must be made in the dynamic response, especially in the control system.

In order to continue with this work, the focus should be on integrating the plant into hybrid microgrid applications. This evolution is aimed at generating synergy with other energy resources such as photovoltaic solar panels and backup batteries. The objective in the continuation of this work is to carry out the integration in an energy management model.

Author Contributions: Conceptualization, L.F.R.-R., C.L.T.-R., N.L.D.-A. and C.R.-C.; formal analysis, L.F.R.-R.; investigation, L.F.R.-R., C.L.T.-R. and N.L.D.-A.; methodology, L.F.R.-R., C.L.T.-R., N.L.D.-A. and C.R.-C.; resources, L.F.R.-R., C.L.T.-R., N.L.D.-A. and C.R.-C.; supervision and validation, L.F.R.-R., C.L.T.-R., N.L.D.-A. and C.R.-C.; writing—original draft preparation L.F.R.-R., C.L.T.-R. and N.L.D.-A.; writing—review and editing, C.L.T.-R., N.L.D.-A. and C.R.-C. All authors have read and agreed to the published version of the manuscript.

Institutional Review Board Statement: Not applicable.

Informed Consent Statement: Not applicable.

Data Availability Statement: Not applicable.

Conflicts of Interest: The authors declare no conflict of interest.

References

1. Herbert, G.M.J.; Krishnan, A.U. Quantifying Environmental Performance of Biomass Energy. *Renew. Sustain. Energy Rev.* **2016**, *59*, 292–308. [CrossRef]
2. Yilmaz, F.; Ozturk, M.; Selbas, R. Design and Thermodynamic Assessment of a Biomass Gasification Plant Integrated with Brayton Cycle and Solid Oxide Steam Electrolyzer for Compressed Hydrogen Production. *Hydrog. Energy* **2020**, *45*, 34620–34636. [CrossRef]
3. Trninić, M.; Stojiljković, D.; Manić, N.; Skreiberg, Ø.; Wang, L.; Jovović, A. A Mathematical Model of Biomass Downdraft Gasification with an Integrated Pyrolysis Model. *Fuel* **2020**, *265*, 116867. [CrossRef]
4. Ordys, A.W.; Pike, A.W.; Johnson, M.A.; Katebi, R.M.; Grimble, M.J. Process Models. In *Modelling and Simulation of Power Generation Plants*; Springer: Berlin/Heidelberg, Germany, 2000; Chapter 4; pp. 144–208.
5. Saravanamuttoo, H.I.H.; Cohen, H.; Rogers, G.F.C. Introduction. In *Gas Turbine Theory*, 5th ed.; Pearson: London, UK, 2013; Chapter 1; pp. 38–44.
6. Jurado, M.F.; Cano, O.A. Capítulo 5 Microturbina de Gas. In *Generación Eléctrica Distribuida Con Microturbina de Gas*; Koobeht International, European Union: Jaén, Spain, 2005; pp. 187–205.
7. Ortega, V.M. Modelado y Simulación Dinámica de Esquemas de Cogeneración. Doctorado Thesis, Universidad Autónoma de Nuevo León, Monterrey, Mexico, 2001.
8. Hussain, A.; Seifi, H. Dynamic Modeling of a Single Shaft Gas Turbine. *IFAC Control. Power Plants Power Syst.* **1992**, *25*, 43–48. [CrossRef]
9. Serrato Monroy, C.C.; Lesmes Cepeda, V. *Metodología Para El Cálculo de Energía Extraída a Partir de La Biomasa En El Departamento de Cundinamarca, Ingeniería*; Universidad Distrital: Bogotá, Colombia, 2016; p. 79.
10. Ramirez Balaguera, L.F.; Barrera Ojeda, D.F. *Potencial Energético de La Biomasa Residual Pecuaria Del Departamento de Cundinamarca–Colombia, Ingeniería*; Universidad Distrital: Bogotá, Colombia, 2017; p. 147.
11. Pozzobon, V.; Salvador, S.; Bézian, J. Biomass Gasification under High Solar Heat Flux_Advanced Modelling_Elsevier Enhanced Reader. *Fuel* **2018**, *214*, 300–313. [CrossRef]
12. Toklu, E. Biomass Energy Potential and Utilization in Turkey. *Renew. Energy* **2017**, *107*, 235–244. [CrossRef]
13. Nunes, L.J.R.; Matias, J.C.O.; Catalão, J.P.S. Biomass in the Generation of Electricity in Portugal: A Review. In *Renewable and Sustainable Energy Reviews*; Elsevier Ltd.: Amsterdam, The Netherlands, 2017; pp. 373–378. [CrossRef]
14. Caliano, M.; Bianco, N.; Graditi, G.; Mongibello, L. Analysis of a Biomass-Fired CCHP System Considering Different Design Configurations. *Energy Procedia* **2017**, *105*, 1683–1691. [CrossRef]
15. Ashok, S.; Balamurugan, P. Biomass Gasifier Based Hybrid Energy System for Rural Areas. In Proceedings of the 2007 IEEE Canada Electrical Power Conference, EPC, Montreal, QC, Canada, 25–26 October 2007; pp. 371–375. [CrossRef]
16. Gómez, B.S. *Diseño e Implementación de Un Sistema de Aprovechamiento de Residuos Orgánicos y Generación de Energía Renovable, Ingeniería*; Universidad ECCI: Bogotá, Colombia, 2017; p. 89.
17. CIGEPI. *Eficiencia de Calderas Para El Uso de Biomasa*; Superintendencia de Industria y Comercio: Antioquia, Colombia, 2017; p. 68.
18. UPME; IDEAM; COLCIENCIAS; UIS. Anexo B Muestreo y Caracterización de La Biomasa Residual En Colombia. In *Atlas del Potencial Energético de la Biomasa Residual en Colombia*; República de Colombia ministerio de Minas y Energía: Bogotá, Colombia, 2013; pp. 131–142.
19. Jiang, R.; Tong Wang, T.; Shao, J.; Guo, S.; Zhu, W.; Jun Yu, Y.; Lin Chen, S.; Hatano, R. Modeling the Biomass of Energy Crops: Descriptions, Strengths and Prospective. *J. Integr. Agric.* **2017**, *16*, 1197–1210. [CrossRef]
20. UPME; Aene. Potencialidades de Los Cultivos Energéticos y Residuos Agrícolas en Colombia. In *Resumen Ejecutivo*; República de Colombia ministerio de Minas y Energía: Bogotá, Colombia, 2003; D.#ANC-631-03,REVISON 1; pp. 98–129.
21. Cao, Y.; Mihardjo, L.W.W.; Dahari, M.; Tlili, I. Waste Heat from a Biomass Fueled Gas Turbine for Power Generation via an ORC or Compressor Inlet Cooling via an Absorption Refrigeration Cycle: A Thermoeconomic Comparison. *Appl. Therm. Eng.* **2021**, *182*, 116117. [CrossRef]
22. Cirillo, D.; Di Palma, M.; La Villetta, M.; Macaluso, A.; Mauro, A.; Vanoli, L. A Novel Biomass Gasification Micro-Cogeneration Plant: Experimental and Numerical Analysis. *Energy Convers. Manag.* **2021**, *243*, 114349. [CrossRef]
23. Elfasakhany Ashraf. Investigation of Biomass Powder as a Direct Solid Biofuel in Combustion. *Ain Shams Eng. J.* **2021**, *12*, 2991–2998. [CrossRef]
24. Hussain, C.M.I.; Norton, B.; Duffy, A. Comparison of Hybridizing Options for Solar Heat, Biomass and Heat Storage for Electricity Generation in Spain. *Energy Convers. Manag.* **2020**, *222*, 113231. [CrossRef]

25. Akrami, E.; Ameri, M.; Rocco, M.V. Developing an Innovative Biomass-Based Power Plant for Low-Carbon Power Production: Exergy and Exergoeconomic Analyses. *Therm. Sci. Eng. Prog.* **2020**, *19*, 100662. [CrossRef]

26. Roy, D.; Samanta, S.; Ghosh, S. Performance Assessment of a Biomass Fuelled Advanced Hybrid Power Generation System. *Renew. Energy* **2020**, *162*, 639–661. [CrossRef]

27. Bisht, A.S.; Thakur, N.S. Small Scale Biomass Gasification Plants for Electricity Generation in India: Resources, Installation, Technical Aspects, Sustainability Criteria & Policy. *Renew. Energy Focus* **2019**, *28*, 112–126. [CrossRef]

28. Sandoval, L.P.; Díaz, C.A. Sustainability Aspects of Biomass Gasification Systems for Small Power Generation. *Renew. Sustain. Energy Rev.* **2020**, *134*, 110180.

29. Herrera, I.; Rodríguez-Serrano, I.; Lechón, Y.; Oliveira, A.; Krüger, D.; Bouden, C. Sustainability Assessment of a Hybrid CSP/Biomass. Results of a Prototype Plant in Tunisia. *Sustain. Energy Technol. Assess.* **2020**, *42*, 100862. [CrossRef]

30. Rey, J.R.C.; Pio, D.T.; Tarelho, L.A.C. Biomass Direct Gasification for Electricity Generation and Natural Gas Replacement in the Lime Kilns of the Pulp and Paper Industry: A Techno-Economic Analysis. *Energy* **2021**, *237*, 321–330. [CrossRef]

31. Krzysztof, S.; Maciej, Z.; Wojciech, G.; Rafal, F. The Operation of a Micro-Scale Cogeneration System Prototype–A comprehensive experimental and numerical analysis. *Fuel* **2021**, *295*, 1–18.

32. Safarian, S.; Ebrahimi Saryazdi, S.M.; Unnthorsson, R.; Richter, C. Artificial Neural Network Integrated with Thermodynamic Equilibrium Modeling of Downdraft Biomass Gasification-Power Production Plant. *Energy* **2020**, *213*, 491–512. [CrossRef]

33. Chiñas-Palacios, C.; Vargas-Salgado, C.; Aguila-Leon, J.; Hurtado-Pérez, E. A Cascade Hybrid PSO Feed-Forward Neural Network Model of a Biomass Gasification Plant for Covering the Energy Demand in an AC Microgrid. *Energy Convers. Manag.* **2021**, *232*, 113896. [CrossRef]

34. Cerinski, D.; Baleta, J.; Mikulčić, H.; Mikulandrić, R.; Wang, J. Dynamic Modelling of the Biomass Gasification Process in a Fixed Bed Reactor by Using the Artificial Neural Network. *Clean Eng. Technol.* **2020**, *1*, 100029. [CrossRef]

35. Ribó-Pérez, D.; Herraiz-Cañete, Á.; Alfonso-Solar, D.; Vargas-Salgado, C.; Gómez-Navarro, T. Modelling Biomass Gasifiers in Hybrid Renewable Energy Microgrids; a Complete Procedure for Enabling Gasifiers Simulation in HOMER. *Renew. Energy* **2021**, *174*, 501–512. [CrossRef]

36. Ahluwalia, K.S.; Domenichini, R. Dynamic Modelling of a Combined Cycle Plant. *ASME* **1989**, *79160*, V004T09A009.

37. Hung, W.W. Dynamic Simulation of Gas-Turbine Generating Unit. *IEE Proc.* **1991**, *138*, 342–350. [CrossRef]

38. Rowen, W.I. Simplified Mathematical Representations of Heavy Duty Gas Turbines. *ASME* **1983**, *105*, 865–869. [CrossRef]

39. Barker, W.; Cronin, M. *Speedtronic Mark IV Control System, Alsthom Gas Turbine Reference Library*. 2000, Volume 4193A. Available online: https://vdocuments.mx/ger-4193a-speedtronic-mark-vi-turbine-control-system-2021-4-6-speedtronica.html?page=1 (accessed on 20 April 2023).

40. Yacobucci, R.B. A Control System Retrofit for a GE Frame 5 Turbine Generator Unit. *IEEE Trans. Energy Convers.* **1991**, *6*, 225–230. [CrossRef]

41. Jurado, F.; Ortega, M.; Cano, A. Neuro-Fuzzy Controller for Gas Turbine in Biomass-Based Electric Power Plant. *Electr. Power Syst. Res.* **2002**, *60*, 123–135. [CrossRef]

42. Zhu, Z.; Wang, X.; Xie, D.; Gu, C. Control Strategy for MGT Generation System. *Energies* **2019**, *12*, 3101. [CrossRef]

43. Jonathan, A.E.; Olubiwe, M.; Okozi, S.O.; Agubor, C.K. Exhaust Temperature Control of Heavy Duty Gas Turbine Due to Incremental Load Demand. *Int. J. Eng. Res. Technol.* **2018**, *7*, 420–426. [CrossRef]

44. Shankar, G.; Mukherjee, V. Load-Following Performance Analysis of a Microturbine for Islanded and Grid Connected Operation. *Int. J. Electr. Power Energy Syst.* **2014**, *55*, 704–713. [CrossRef]

45. El-Sharif, I.A.; El-Fandi, M.M. Micro Gas Turbine Simulation and Control. In Proceedings of the Conference for Engineering Sciencies and Technology (CEST), Castelverde, Libya, 25–27 September 2018; pp. 1–10.

46. Shakur, S.A.; Jain, S.K. Micro-Turbine Generation Using Simulink. *Int. J. Electr. Eng.* **2012**, *5*, 95–110.

47. Guda, S.R.; Wang, C.; Nehrir, M.H. Modeling of Microturbine Power Generation. *Electr. Power Compon. Syst.* **2006**, *34*, 1027–1041. [CrossRef]

48. Singh, N.K.; Tiwari, P.; Srivastava, J. Simulation Of Microturbine Generation System For Unbalance Grid Power. *Int. J. Eng. Res. Technol.* **2013**, *2*, 967–974.

49. Abdollahi, S.E.; Vahedi, A. Dynamic Modelling of Micro-Turbine Generation Systems Using Matlab/Simulink. *Renew. Energy Power Qual. J.* **2005**, *1*, 146–152. [CrossRef]

50. Herrador, C.M. *Modelado En Matlab-Simulink de Generadores Eléctricos Conectados a La Red*; Universidad de Sevilla: Sevilla, Spain, 2016.

51. Chiguano, B.A. Estimación de Parámetros Eléctricos de La Máquina Sincrónica Utilizando Matlab-Simulink. Bachelor's Thesis, Escuela Politecnica Nacional, Quito, Ecuador, 2018.

52. Sistemas de Generación. Generadores Síncronos y Asíncronos. Available online: https://biblus.us.es/bibing/proyectos/abreproy/4991/fichero/4+Sistemas+de+generaci%C3%B3n.pdf (accessed on 4 April 2023).

53. Sistema Interconectado Nacional. Indicadores de Pronósticos Oficiales de Demanda. Available online: https://www.xm.com.co/consumo/informes-demanda/indicadores-de-pronosticos-oficiales-de-demanda (accessed on 2 April 2023).

54. Consejo Nacional de Operaciones-CNO. Acuerdo 1303 Por el Cual se Actualizan los Procedimientos Para la Gestión Integral de la Demanda. Available online: https://www.cno.org.co/content/acuerdo-1303-por-el-cual-se-actualizan-los-procedimientos-para-la-gestion-integral-de-la (accessed on 2 April 2023).
55. Enel-Codensa. Innovación y Sostenibilidad. Available online: https://www.enel.com.co/es/medio-ambiente-desarrollo-sostenible.html (accessed on 2 April 2023).